SAND2009-4532C

Gamma-Radiation-Induced Photodarkening in Actively Pumped Yb^{3+}-Doped Optical Fiber and Investigation of Post-Irradiation Transmittance Recovery

B. P. Fox[a], K. Simmons-Potter[a], S. W. Moore[b], J. H. Fisher[c], and D. C. Meister[d]
[a]University of Arizona, Tucson, AZ 85721
[b]Sandia National Laboratories, Livermore, CA 94551
[c]GH Systems Inc., Huntsville, AL 35758
[d]Sandia National Laboratories, Albuquerque, NM 87123

ABSTRACT

Fibers doped with rare-earth constituents such as Yb^{3+} and Er^{3+}, as well as fibers co-doped with these species, form an essential part of many optical systems requiring amplification. This study consists of two separate investigations examining the effects of gamma-radiation-induced photodarkening on the behavior of rare-earth doped fibers. In one part of this study, an Yb^{3+}-doped fiber was actively pumped by a laser diode during a gamma-radiation exposure to simulate the operation of an optical amplifier in a radiation environment. The response of the amplified signal was observed and monitored over time. In the other part of this study, a suite of previously irradiated rare-earth doped fibers was heated to an elevated temperature of 300°C and the transmittance monitored over an 8-hour period. Transmittance recoveries of ~10 - 20% were found for Er^{3+}-doped fiber, while recoveries of ~5 - 15% and ~20% were found for Yb^{3+}- and Yb^{3+}/Er^{3+} co-doped fibers, respectively.

Keywords: Rare-earth doped fibers, photodarkening, radiation-induced absorption, gamma irradiation, fiber loss recovery, fiber annealing, elevated-temperature thermal anneal, Yb-doped fiber amplifier

1. INTRODUCTION

The extensive presence of fiber-optics in modern systems largely stems from the high-bandwidth capabilities and high reliability of this technology. For these reasons, an ever-increasing effort has been made in recent times to use fiber-optics in highly specialized applications, including systems operating in radiation environments. Such adverse radiation environments are diverse and range from nuclear to space environments. The monolithic structure of these fibers leads to high-reliability and their low weight and small volume are further qualities that make them desirable for systems operating in adverse-radiation conditions.

This particular research effort studies the effect of gamma radiation on rare-earth doped optical fibers. Fibers doped with these rare-earth constituents are of particular interest, since they often serve as the most important part of a fiber optic system due to their high-power capabilities, and are often the most sensitive part of this system[1-6]. The types of doped fibers that will be investigated in this paper are Yb^{3+}-, Er^{3+}-, as well as Yb^{3+}/Er^{3+} co-doped fibers. The first ion has a simple band structure, which can be used to amplify signals in the ~1.06 μm region, while the second is extensively used in applications due to its ability to amplify in the low-loss ~1.53 μm operating region of optical fibers[7-11]. The co-doped fibers combine high absorption efficiency of the Yb-ion with the favorable output amplification region of the Er-ion, thereby creating a fiber which is highly desirable in many applications[12-15].

When optical fibers are exposed to gamma radiation, a photodarkening process takes place in which the optical transmittance of the fiber decreases with increasing accumulated dose. Understanding this process is of great importance, since it increases the predictability of fiber behavior, improving designs for systems operating in radiation environments. The physical origin of the darkening is the presence of trap states, which are filled as a consequence of radiation, leading to an unwanted increase of absorption of light at relevant wavelengths, such as the signal and pump

wavelength of an amplifier[16-22]. Photodarkening thus manifests itself as a light loss through passive fibers, leading to overall output power reductions of fibers connected in amplifier configurations[23-26].

The amount of absorption present is contingent upon a large number of factors, ranging from the fiber geometry, fabrication methods, and type of glass, to specific type and amounts of dopants, as well as type of radiation, dose rate, and total accumulated dose[27-37]. Temperature furthermore plays a significant role in the kinetics of absorption centers, one of the important effects being the ability to reverse the radiation-induced absorption using elevated-temperature anneals[13, 20, 38]. The thermal energy, if significant enough, can release the electron out of a given trap, thereby dissolving the absorption associated with that center. The effect of thermal anneals on rare-earth doped fibers is the focus of the first part of this study, since it is relevant to both the underlying physics as well as the engineering aspect of fiber optic design. It is important to emphasize that elevated temperatures could potentially be designed into a given system as a mode of operation.

From the perspective of system design for applications in environments such as space, the effect of radiation on rare-earth doped fibers in an active amplifier system is paramount, which is why the second part of this study investigates the output of an Yb^{3+}-doped fiber amplifier with the active rare-earth doped fiber spool under irradiation. In terms of the radiation-induced degradation, the presence of pump photons in the amplifier allows for the possibility of more complex processes in contrast to the ones present in the passive rare-earth doped fibers, so evidence of the presence of such processes will be looked for.

2. EXPERIMENT

2.1 Fiber Anneals

To study the effect of annealing on rare-earth-doped fibers, a suite of Yb^{3+}- and Er^{3+}-doped aluminosilicate fibers from Liekki and Nufern that had previously been irradiated during earlier sets of experiments was subjected to elevated temperatures. The initial irradiations had been passive (i.e. the fibers had not been pumped), and for the exposure, a Co^{60} source from the Gamma Irradiation Facility (GIF) at Sandia National Laboratories, New Mexico, had been used. Since the experiments had looked at a myriad of different irradiation conditions, the primary focus of the anneals was to find out whether or not, as well as and how much, recovery of lost transmittance was possible. An exhaustive study of the relation between irradiation conditions and recovery was not attempted, as more repeatability would have been required.

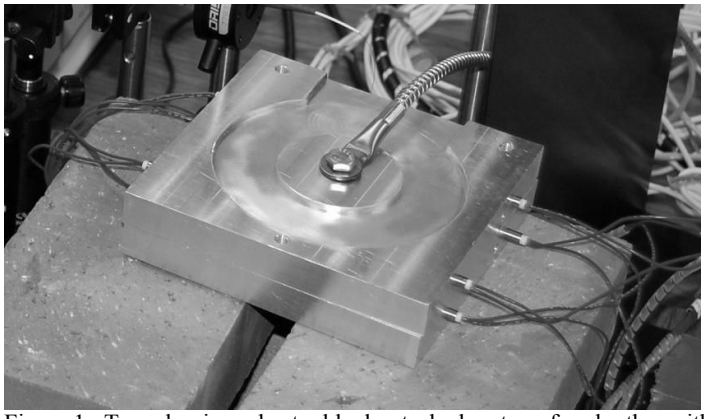

Figure 1: Two aluminum heater blocks stacked on top of each other with the rare-earth doped fibers (not seen in picture) coiled inside a milled part of the lower heater in between the two heaters shown. Picture also shows location of heating elements, as well as one of the locations of one of the thermocouple (the other being underneath the lower heater).

Anneals were conducted at least one month after initial irradiations had taken place. The annealing experiments consisted of guiding broad-band reference light from a xenon arc lamp through a collimating lens and a focusing lens into one of the connectorized ends of the rare-earth doped fiber. The light exiting the other end of the fiber was then guided into an optical spectrometer (Ocean Optics NIR 512). The rare-earth-doped sample fibers were then coiled to a diameter under 5" and placed into a groove milled into an aluminum heater (Figure 1), to which heat was transferred via four cartridge heaters. To keep the fiber in place while ensuring uniform heating, another heater with four cartridge heaters was placed on top of the one containing the fiber. A maximum temperature of 300°C was chosen and said temperature was kept constant for 8 hours, after which the heaters were turned off until temperatures close to room temperature were achieved. Spectra throughout the entire experiment were taken in the near infrared at regular time intervals (~12 mins) and associated temperatures were recorded with the spectra. An analysis of the effect of post-irradiation annealing was then performed.

2.2 Active Amplifier Irradiation

In the second part of this study, an Yb^{3+}-doped optical fiber from Liekki was actively pumped in an amplifier configuration and monitored in situ during a radiation exposure from a Co^{60} source at the Leach Science Center in Auburn, AL. A schematic of the experimental setup is given in Figure 2 (a). The amplifier was composed of passive fiber, an Yb^{3+}-doped optical fiber, a Micro Laser Systems Fermion I probe laser at ~1.06 μm, and a pump laser diode radiating at 916 nm and operating near 2 V. The pump light was coupled into an optical isolator, and the two laser beams were then unified into a single delivery fiber using a combiner. The delivery fiber was a passive, undoped 20/123DC fiber from Liekki, which propagated the signal and pump beams through a conduit into the gamma irradiation cell. The passive fiber was then fusion spliced to ~3 m of active Yb^{3+}-doped Yb1200-20/125DC fiber from Liekki, the first number designating the nominal peak absorption at 976 nm in the core in dB/m, and the second and third numbers denote the core and cladding diameters, respectively, in μm. The 'DC' specifies double-clad fibers. The active fiber, which was spooled and mounted vertically to assure uniform irradiation, was positioned such that there was as little of the passive fiber as possible protruding out of the conduit port hole, the intention being to avoid darkening of the passive fiber to assure that the radiation-induced processes would only be present in the active fiber portion of the amplifier. The second end of the Yb^{3+}-doped spool was fusion spliced to another passive 20/123DC fiber, which guided the output of the amplifier out of the test cell and onto a 3Σ Coherent detector, which was configured for the manual monitoring of the probe wavelength of ~1.06 μm.

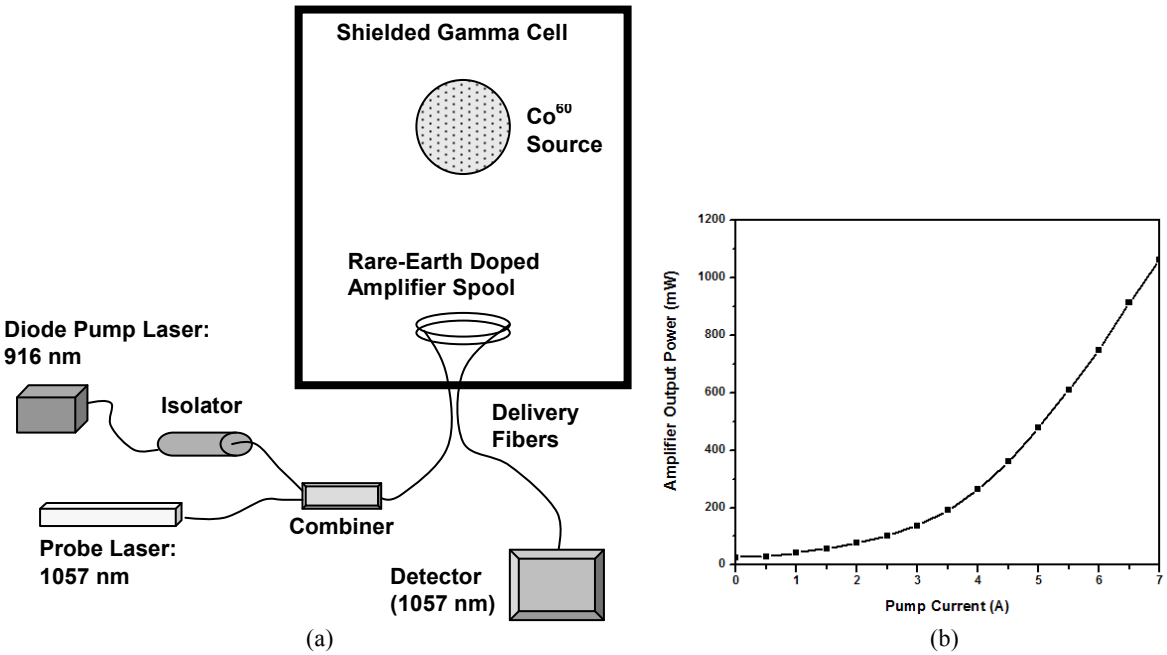

Figure 2: (a) Gamma test cell at Auburn University, Auburn, AL. (b) Amplifier output power at ~1.06 μm vs. diode drive current plot before gamma-radiation exposure.

To operate the amplifier, the probe laser was adjusted to give the maximum amplifier output, and the current driving the pump diode was kept at 6 A throughout the experiment, the only exceptions occurring while tracing output power vs. diode drive current curves. Figure 1 (b) shows one such curve taken before commencing the irradiation. It should be noted that the amplifier output power at all diode drive currents was much greater before the amplifier was passed through a conduit into the gamma test cell, a consequence likely due to stresses induced in the fiber due to tight turns of the conduit. Within the shielded gamma cell, the individual Co^{60} elements were arranged on a platform, which was raised out of a pool of water when the irradiation was to begin. The source array was found to yield a dose rate of approximately 419 rad(Si)/hr, which was determined as the average of a Geiger-Müller counter measurement (~440 rad(Si)/hr) and a measurement using an array of thermoluminescent devices (TLDs, yielding ~400 rad(Si)/hr on average).

3. RESULTS

2.1 Fiber Anneals

Before the anneals were conducted, all fibers were irradiated by a Co^{60} source, leading to substantial radiation-induced photodarkening[39]. Figure 3 depicts the recovered loss from a representative Er^{3+}-doped fiber, the lower line showing the wavelength-dependent transmittance after irradiation normalized relative to the transmittance of the pre-irradiated fiber, and the upper line showing the transmittance of the fiber after the 8 hour, 300°C elevated-temperature anneal (on the same scale). It can clearly be seen that the average recovery of this fiber is on the order of 20%, and that the recovery is clearly non-uniform with respect to wavelength, with the least amount of recovery observed at the extrema of the measurement window (below 1.0 μm and close to 1.7 μm). Figures 4 (a) depicts the change of transmittance relative to the initial post-irradiation transmittance for various temperatures during the heat-up phase, while Figure 4 (b) shows the change in transmittance for different times during the 8 hour soak relative to the initial transmittance spectrum corresponding to when the temperature reached 300°C. The former plot indicates that significant recoveries of transmittance loss are attained at a temperature of 270°C, with temperatures below ~200°C actually showing a decrease in transmittance. While the heat-up phase yields a little more than one half of the final transmittance recovery of the Er^{3+}-doped fiber, the rest is obtained during the 8 hour soak, shown in the latter plot. Only a minute amount of transmittance recovery was obtained during the cool-down phase (not depicted). Looking at the entire suite of heated fibers doped with Er-ions, the average transmittance recovery was ~15-20%.

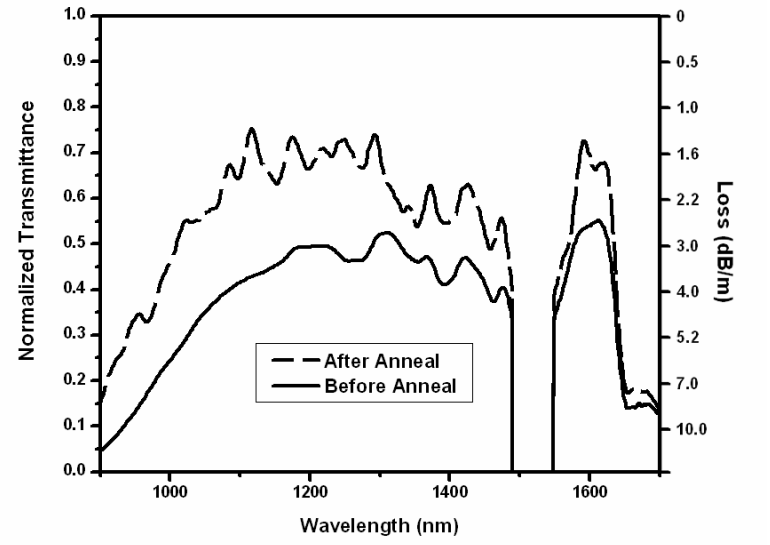

Figure 3: Transmittance of a gamma-radiation photodarkened Liekki Er16-8/125 fiber before and after 8 hour thermal anneal (see section 2.2 for fiber designations). Values are normalized to pre-irradiated transmittance.

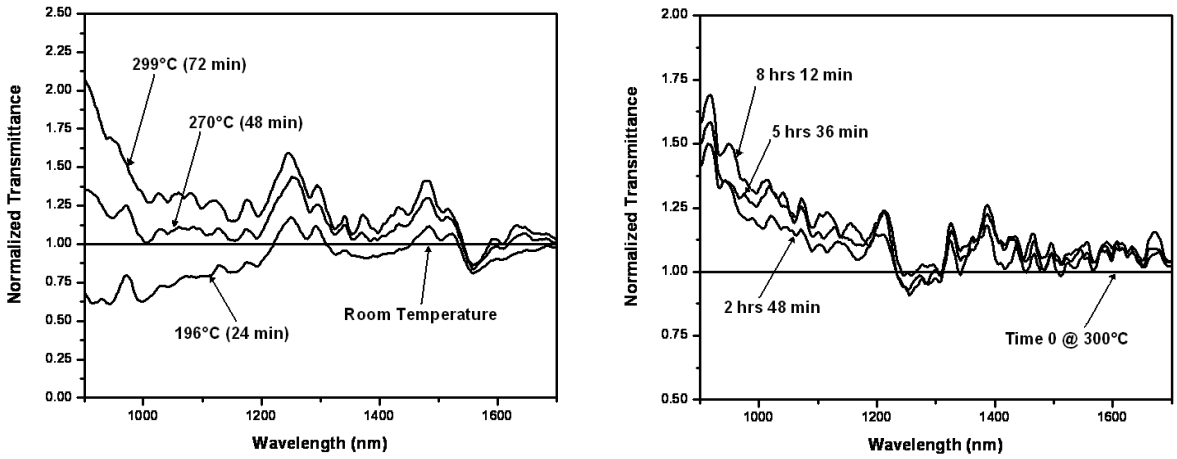

(a) (b)

Figure 4: Transmittance of Liekki Er16-8/125 fiber at different temperatures and anneal times. Plot (a): heat-up phase, normalized relative to initial pre-anneal but post-irradiation transmittance values (note: heat-up times are also shown). Plot (b): 8 hr soak, normalized relative to first transmittance spectrum that reached the temperature of 300ºC.

Figure 5 depicts the recovered loss in a representative Yb^{3+}-doped fiber after the 300°C anneal. It can clearly be seen that the transmittance increased about 15% across the spectrum, with most of the recovery occurring away from the extremes of the measured wavelength window, as in the Er^{3+}-doped fiber. Figure 6 shows the recovery observed during (a) the heat-up phase, and (b) the cooling-down phase of the elevated-temperature anneal experiment. It is evident that the majority of the transmittance was recovered during the heat-up phase of the experiment, and a close look at the data set reveals that significant transmittance recovery is only seen at temperatures above ~250°C. An interesting feature just below the wavelength of 1.1 μm in Figure 6 is noteworthy: When the fiber is heated up, the transmittance here decreases to about one-half the original value (Figure 6 (a)); but as the fiber cools, the transmittance increases by a factor of about two (Figure 6 (b)), thereby representing a temperature reversible absorption center. Other Yb^{3+}-doped fibers showed less recovery, with all transmittance recoveries falling in the range of ~5-15%, as well as a less pronounced temperature dependent absorption at 1.1 μm.

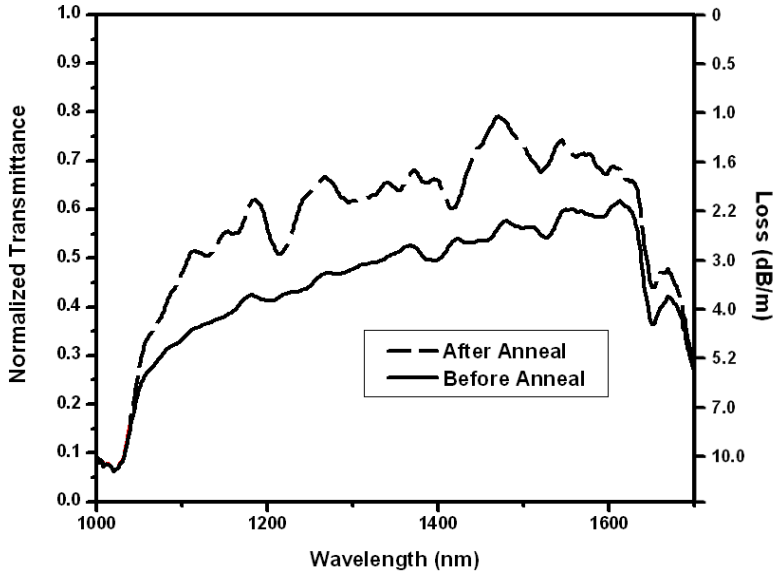

Figure 5: Transmittance of a Liekki Yb1200-4/125 fiber before and after 8 hour thermal anneal (values normalized to pre-irradiated transmittance).

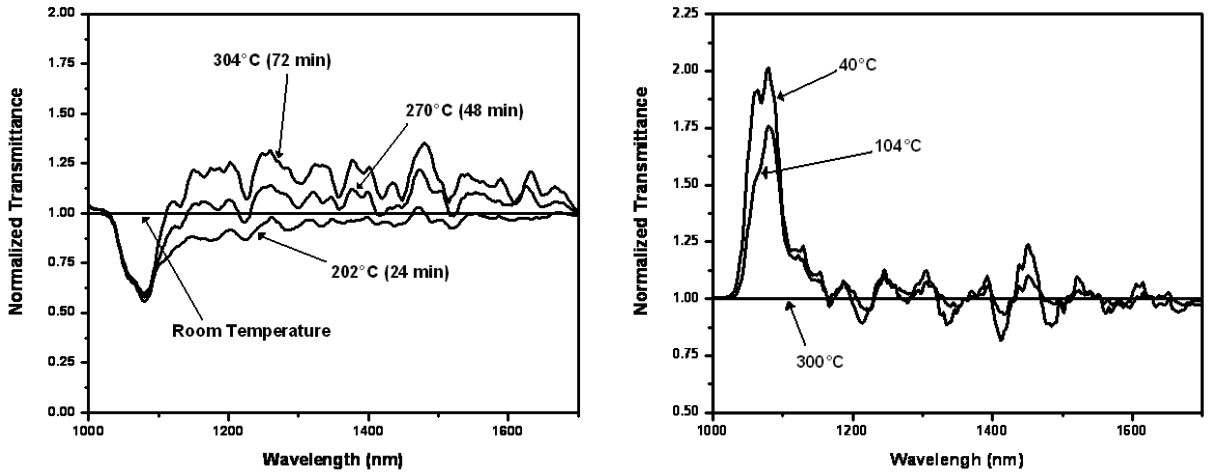

Figure 6: Transmittance of a Liekki Yb1200-4/125 fiber at different temperatures and anneal times. Plot (a): heat-up phase, normalized relative to initial pre-anneal but post-irradiation transmittance values. Plot (b): cooling phase, normalized relative to last transmittance spectrum with temperature of 300ºC before heaters were turned off.

The result of annealing an Er^{3+}/Yb^{3+}-co-doped fiber is shown in Figure 7. The largest normalized transmittance increase in the entire data set is observed in this sample, at a wavelength of just over 1.6 μm, where an increase of ~30% is observed. Although this sample experiences a large average recovery of ~20%, much like the Er^{3+}-doped fibers, the general annealing behavior bears more resemblance to the Yb^{3+}-doped fiber, exhibiting no initial decrease of transmittance at lower temperatures, and showing the same temperature-dependent, reversible absorption at ~1.1 μm.

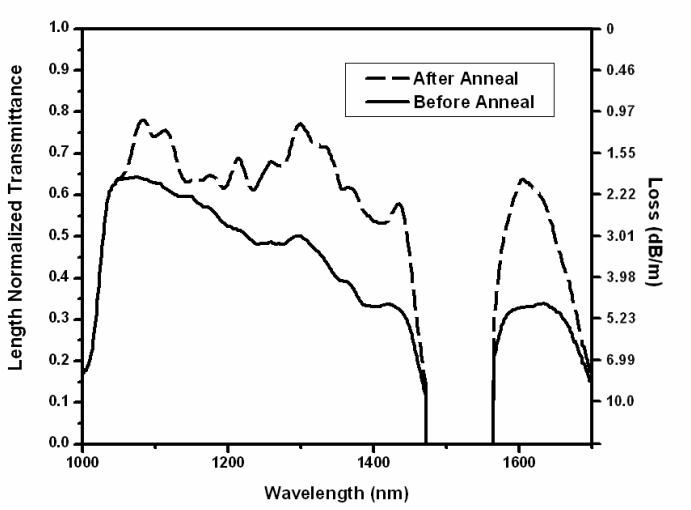

Figure 7: Transmittance of a Nufern multi-mode EYDF-12/130-HE Er^{3+}/Yb^{3+} fiber before and after 8 hour thermal anneal (values normalized to pre-irradiated transmittance).

2.2 Active Amplifier Irradiation

The radiation exposure of the active amplifier consisted of several short irradiation periods with one long irradiation taking place at the end, all carried out using a 6 A diode drive current. The initial short irradiation periods were a consequence of radiation measurement apparatus such as TLDs being brought into and out of the radiation cell and

another concurrent experiment being run. The result of the last irradiation is depicted in Figure 8, plotted as amplifier output at the probe wavelength of 1.057 μm in mW vs. dose, with approximately ~7.6 krad(Si) of dose being accumulated during this period. Periods during which the source was lowered and the irradiation stopped (e.g. to remove TLDs) did not result in any annealing of the radiation amplifier performance degradation, nor did the 2 hour post-irradiation period after the experiment, also depicted in Figure 8. All data was recorded manually, leading to gaps in the plot in Figure 8, but the data still shows a clear exponential decrease of amplifier output power from ~780 mW to ~137 mW, emphasized with an exponentially shaped curve fitted to the data points obtained during the final irradiation. The power loss indicated by the fitted curve is approximately 1 dB/krad(Si).

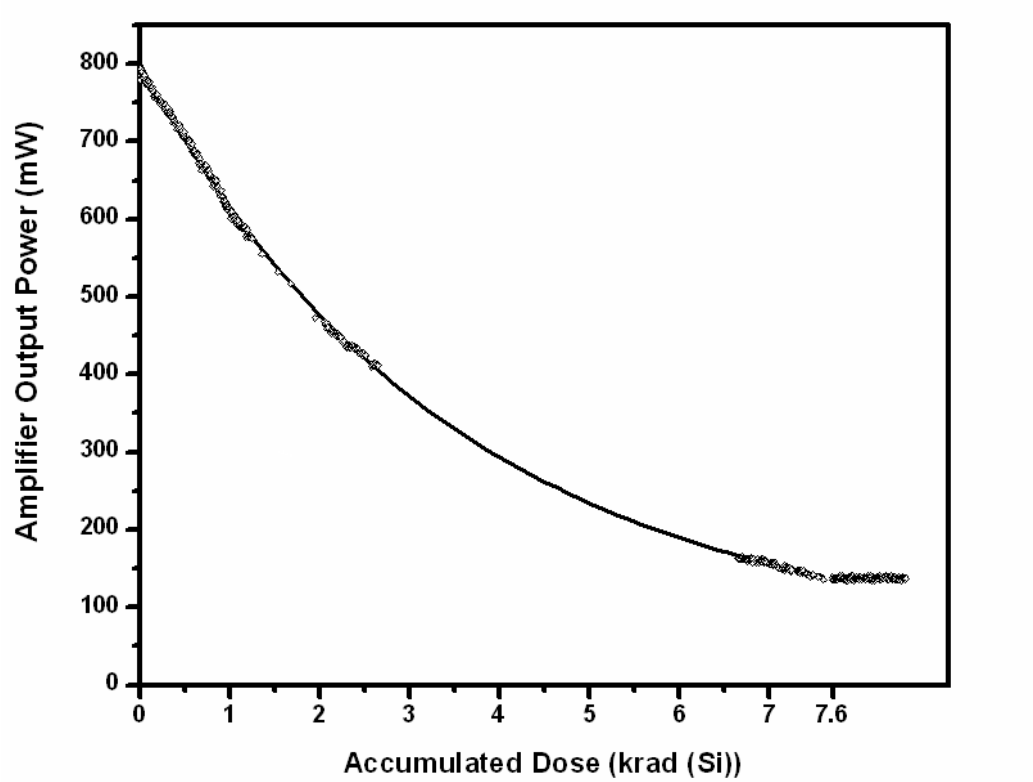

Figure 8: Decrease of amplifier output power at ~1.06 μm vs. total accumulated radiation dose. The source was lowered after a dose of about 7.6 krad(Si), and post-irradiation data is also shown. The exponential curve was fitted to the data points during the irradiation. The dose rate was ~419 rad(Si)/min.

Figure 9 depicts the amplifier output power vs. diode pump current for various accumulated doses up to 7.6 krad(Si), after which the curves remains constant. The monotonic decrease in amplifier output power at all pump currents clearly shows the degradation of the amplifier performance. It should be noted that the amplifier output power vs. diode drive current plot before any irradiation took place (Figure 2 (b)) is not plotted in Figure 9, because there were several short previous irradiations and some changes in amplifier output power were observed prior to the commencement of the final irradiation period. These can be attributed to the amplifier untwisting and settling in the conduit, since guiding the amplifier through the conduit required much bending of the amplifier, affecting the amplifier output power. Based on the amplifier output power at a diode drive current of 6 A before any radiations exposures and before the final irradiation, however, it can be surmised that the plot of Figure 2 (b) should be very close to the initial curve of 0 krad(Si) of Figure 9 (the initial powers are ~780 mW for the latter vs. ~790 mW for the former).

To gain physical insight into the process of photodarkening, data with the pump diode current set at 0 A was taken over an accumulated dose of ~5.4 krad(Si). Although there are uncertainties with respect to the detector, the data normalized to a 1 m fiber length suggests a transmittance decrease at ~1.06 μm of around ~15%, which is very close to what was found in previous passive irradiations with similar Yb^{3+}-doped fibers, suggesting that generation of color centers at the pump wavelength are of primary concern with respect to amplifier performance[22].

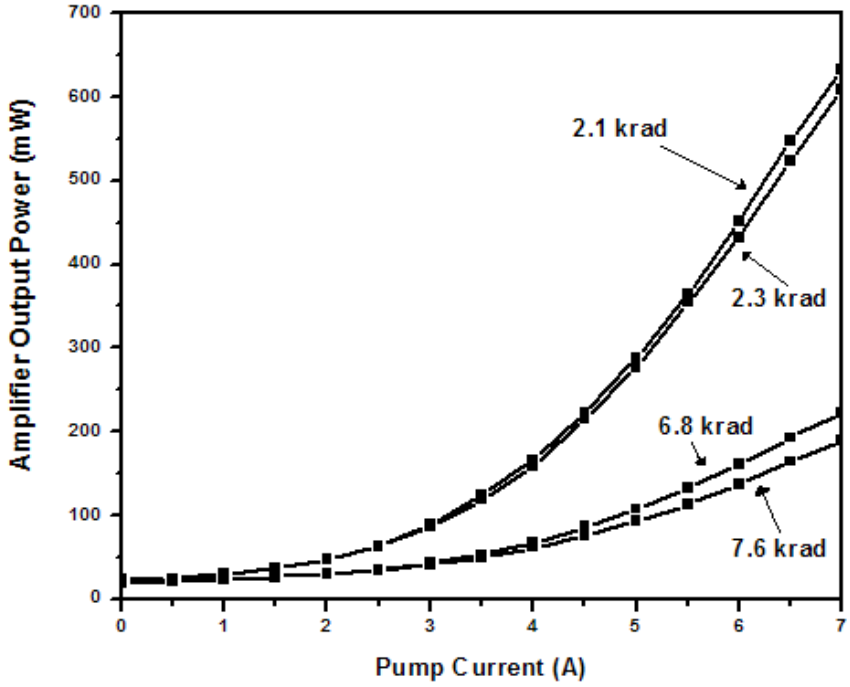

Figure 9: Amplifier output power at 1.057 μm vs. diode drive current for various total accumulated radiation doses during the final irradiation period under a dose rate of ~419 rad(Si)/min.

4. CONCLUSION

Two studies were conducted pertaining to the operation of rare-earth doped amplifiers in radiation environments. In the first part, thermal annealing of gamma-irradiated rare-earth optical fibers was conducted to determine the degree to which photodarkening can be reversed. In the second part, the effects of gamma radiation on an actively-pumped Yb^{3+}-doped amplifier were examined to assess the degree of degradation in performance. The design of an optical amplifier system relies on the understanding of the behavior of the amplifier in various operational modes, and both experiments give valuable insight into possible operational modes for an optical amplifier system. The specific modes investigated in this study are the amplifier is being pumped continuously, as well as the amplifier fiber is being annealed via heaters while not operating.

With regard to the annealing experiments it was found that the photodarkened fibers exhibited transmittance recovery following the 8 hour, 300°C thermal anneal. The recoveries were non-uniform across the measured wavelength window from ~1.0 μm to 1.7 μm and ranged from ~5-20% on average, with Er^{3+}-doped fiber showing average transmittance increases of ~15-20%, Yb^{3+}-doped fibers showing increases of ~5-15%, and the Er^{3+}/Yb^{3+}-doped fiber showing increases of ~20%. Significant recovery was only found when the fibers were heated above ~250°C, and the literature suggests that complete photodarkening recovery might only be possible at even higher temperatures[38]. In the Er^{3+}-doped fibers, a little more than half of the recovery was obtained during the heating period alone, with most of the remaining recovery being attained during the 8 hour soak. The Yb^{3+}-doped fibers, by contrast, tended to experience most of the recovery during the heating phase, with more moderate recoveries during the soak and cooling down phases. The Yb^{3+}-doped fiber samples also showed a temperature-dependent, reversible absorption at wavelengths just below 1.1 μm, in which an elevated temperature of 300°C leads to a reduction in transmittance, while cooling the sample fiber down returned the transmittance to or close to its pre-heated state. All in all, the fiber transmittance recovery data is important with respect to the design of systems operating in ionizing radiation environments, as well as from the standpoint of giving insight into basic processes of rare-earth doped fibers.

With regard to the active amplifier irradiation experiment, the data showed an exponential decrease in amplifier output power at the signal wavelength incurred by the radiation environment. Plotting amplifier output power vs. diode pump current showed a monotonic decrease of the power at all drive currents, which was not found to anneal in a 2 hour source-free room temperature anneal. A closer look at the transmittance of the 1.06 μm signal wavelength indicates a decrease of ~16%, which is commensurate with values obtained in previous passive Co^{60} exposures of similar Yb^{3+}-doped fibers. This suggests that the absorption centers responsible for the decrease of transmittance at the signal wavelength is neither affected by the presence of the signal wavelength nor by the presence of the 916 nm pump wavelength. Especially the latter is an important result, since it indicates that the formation of absorption centers at the pump wavelength are of primary importance concerning the performance of the amplifier as opposed to the formation of absorption centers at the signal wavelength. Thus, the data presented here indicates that the degradation of amplifier performance can be attributed to a decrease in energy transfer efficiency from the pump wavelength to the lasing wavelength, caused by the formation of absorption centers at the pump wavelength. This highlights the importance of closely investigating the pump wavelength in order to improve performance, lifetime, and reliability of the Yb^{3+}-doped amplifier.

Rare-earth doped optical fiber amplifier systems are sensitive to radiation environments, and the results of this study are valuable to the design of amplifier systems in regard to withstanding gamma radiation. The data within this publication indicates that radiation hardening of the amplifier requires material engineering of the active rare-earth doped fiber material, in particular with regard to the prevention of absorption centers related to the pump wavelength. With respect to a possible thermal annealing mode of operation during which the amplifier is turned off, it can be said that a minimum temperature must be reached (~250°C). The soak time of the anneal is of less importance in an Yb^{3+}-doped fiber than in an Er^{3+}-doped fiber, since the former experiences most of the recovered transmittance during the heat-up phase of the anneal. Although the data presented gives insight into optical amplifier design issues for radiation environments, further research in the area of amplifier degradation mechanisms is necessary to allow for the design of specific applications.

5. ACKNOWLEDGEMENTS

The authors would like to thank Dahv A. V. Kliner for his assistance and for the active fiber harness design, Max Cichon, Engineering Associate at Auburn University, for his help with the gamma radiation facility, and Richard Horton at GH systems for co-ordinating experimental scheduling. This work was primarily supported by the University of Arizona and the State of Arizona TRIF funds, and in partly by Laboratory Directed Research and Development, Sandia National Laboratories, under contract DE-AC04-94AL85000.

6. REFERENCES

1. R. L. Farrow, D. A. V. Kliner, P. Schrader, A. A. Hoops, S. W. Moore, G. R. Hadley, and R. L. Schmitt, "High-Peak-Power (>1.2 MW) Pulsed Fiber Amplifier," *Proc. SPIE* **6102**, 61020L, 2006.
2. K. Sumimura, H. Yoshida, H. Fujita, and M. Nakatsuka, "Yb Fiber Mode-Locked Laser with a Wide Tuning Range for Chirped Pulse Amplification System," *IEICE Electronics Express* **3** (11), pp. 233-237, 2006.
3. Y. Jeong, J. K. Sahu, D. N. Payne, and J. Nilsson, "Ytterbium-Doped Large-Core Fiber Laser with 1.36 kW Continuous Wave Output Power," *Opt. Exp.* **12** (25), pp. 6088-6092, 2004.
4. C. D. Brooks and F. Di Teodoro, "1-mJ Energy, 1-MW Peak-Power, 10-W Average-Power, Spectrally Narrow, Diffraction-Limited Pulses From a Photonic-Crystal Fiber Amplifier," *Opt. Exp.* **13** (22), pp. 8999-9002, 2005.
5. M. Laroche, H. Gilles, S. Girard, N. Passilly, and K. Aït-Ameur, "Nanosecond Pulse Generation in a Passively Q-Switched Yb-Doped Fiber Laser by Cr^{4+}:YAG Saturable Absorber," *IEEE Photonics Technology Letters* **18** (6), pp. 764-766, 2006.
6. R. J. Bussjager, M. J. Hayduk, S. T. Johns, and E. W. Taylor, "Comparison of Radiation-Induced Passive and Dynamic Responses in Two Erbium-Doped Fiber Lasers," *IEEE Aerospace Conf. Proc.* **3**, pp. 1369-1379 2002.
7. R. Paschotta, J. Nilsson, A. C. Tropper, and D. C. Hanna, "Ytterbium-Doped Fiber Amplifiers," *IEEE J. Quantum Electron.* **33** (7), pp. 1049-1056, 1997.

8. H. M. Pask, R. J. Carman, D. C. Hanna, A. C. Tropper, C. J. Mackechnie, P. R. Barber, and J. M. Dawes, "Ytterbium-Doped Silica Fiber Lasers: Versatile Sources for the 1-1.2 μm Region," *IEEE Journal of Selected Topics in Quantum Electronics* **1** (1), pp. 2-13, 1995.
9. J. L. Zyskind, "Erbium-Doped Fiber Amplifiers," *Proc. SPIE* **158**, pp. 14-23, 1991.
10. W. J. Miniscalco, "Erbium-Doped Glasses for Fiber Amplifiers at 1500 nm," *J. Lightwave Technology* **9** (2), pp. 234-250, 1991.
11. E. W. Taylor, S. J. McKinney, A. D. Sanchez, J. E. Winter, D. M. Craig, A. H. Paxton, R. Ewart, K. Miller, T. O'Connor, and R. Kaliski, "Gamma-Ray Induced Effects in Erbium-Doped Fiber Optic Amplifiers," *Proc. SPIE* **3440**, pp. 16-23, 1998.
12. J. Nilsson, S.-U. Alam, J. A. Alvarez-Chavez, P. W. Turner, W. A. Clarkson, and A. B. Grudinin, "High-Power and Tunable Operation of Erbium-Ytterbium Co-Doped Cladding-Pumped Fiber Lasers," *IEEE J. of Quantum Electron.* **39** (8), pp. 987-994, 2003.
13. R. G. Ahrens, J. J. Jaques, M. J. LuValle, D. J. DiGiovanni, and R. S. Windeler, "Radiation Effects on Optical Fibers and Amplifiers," *Proc. SPIE* **4285**, pp. 217-225, 2001.
14. R. G. Ahrens, J.A. Abate, J. J. Jaques, H. M. Presby, A. B. Fields, D. J. DiGiovanni, R. S. Windeler, S. Kannan, and M. J. LuValle, "Radiation Reliability of Rare Earth Doped Optical Fibers for Laser Communication Systems," *Proc. MILCOM '99, IEEE* **1**, pp. 694-697, 1999.
15. J. E. Townsend, W. L. Barnes, K. P. Jedrzejewski, and S. G. Grubb, "Yb^{3+} Sensitised Er^{3+} Doped Silica Optical Fibre with Ultrahigh Transfer Efficiency and Gain," *Electron. Lett.* **27** (21), pp. 1958-1959, 1991.
16. D. L. Griscom, M. E. Gingerich, and E. J. Friebele, "Radiation Induced Defects in Glasses: Origin of Power-Law Dependence of Concentration on Dose," *Phys. Rev. Lett.* **71** (7), pp. 1019-1022, 1993.
17. D. L. Griscom, "Nature of Defects and Defect Generation in Optical Glasses," *Proc. Soc. Photo-Opt. Instrum. Eng.* **541**, 1985.
18. P. Borgermans, B. Brichard, and M. Decréton, "Models for the Radiation Induced Attenuation in Pure Silica Optical Fibres: Spectral Dependencies and Absorption Band Kinetics," *Proc. SPIE* **4547** (53), pp. 53-60, 2002.
19. O. Berné, M. Caussanel, and O. Gilard, "A Model for the Prediction of EDFA Gain in a Space Radiation Environment," *Photonics Technology Letters, IEEE* **16** (10), pp. 2227–2229, 2004.
20. J. D. O. McFadden, R. Greenwell, J. Hatch, C. Barnes, D. Pentrack, and D. Scott, "Measurements and Results of Gamma Radiation Induced Attenuation at 980 nm of Single Mode Fiber," *Proc. SPIE* **2811**, pp. 77-86, 1996.
21. B. P. Fox, Z. V. Schneider, K. Simmons-Potter, W. J. Thomes, D. C. Meister, R. P. Bambha, D. A. V. Kliner, and M. J. Söderlund, "Gamma Radiation Effects in Yb-Doped Optical Fiber," *Proc. SPIE* **6453**, 2007.
22. B. P. Fox, Z. V. Schneider, K. Simmons-Potter, W. J. Thomes, D. C. Meister, R. P. Bambha, and D. A. V. Kliner, "Spectrally-Resolved Transmission Loss in Gamma Irradiated Yb-Doped Optical Fibers," *IEEE J. of Quantum. Electron.* **44** (6), pp. 581-586, 2008.
23. M. Alam, J. Abramczyk, P. Madasamy, W. Torruellas, and A.Sanchez, "Fiber Amplifier Performance in γ–Radiation Environment," *OFC/NFOEC Conf.*, pp. 1-3, 2007.
24. E. W. Taylor and J. Liu, "Ytterbium-Doped Fiber Laser Behavior in Gamma-Ray Environment," *Proc. SPIE* **5897**, 58970E, 2005.
25. M. Van Uffelen, S. Girard, F. Goutaland, A. Gusarov, B. Brichard, and F. Berghmans, "Gamma Radiation Effects in Er-Doped Silica Fibers," *IEEE Trans. Nucl. Sci.* **51** (5), pp. 2763-2769, 2004.
26. T. S. Rose, D. Gunn, and G. C. Valley, "Gamma and Proton Radiation Effects in Erbium-Doped Fiber Amplifiers: Active and Passive Measurements," *J. Lightwave Technology* **19** (12), pp. 1918-1923, 2001.
27. B. Tortech, Y. Ouerdane, S. Girard, J.-P. Meunier, A. Boukenter, T. Robin, B. Cadier, and P. Crochet, "Radiation Effects on Yb- and Er/Yb-Doped Optical Fibers: A Micro-Luminescence Study," *J. Non-Cryst. Solids* **355** (18-21), pp. 1085-1088, 2009.
28. T. Arai, K. Ichii, S. Tanigawa, and M. Fujimaki, "Defect Analysis of Photodarkened and Gamma-Ray Irradiated Ytterbium-Doped Silica Glasses," *Optical Fiber Communication Conference, OSA Technical Digest*, paper OWT2, 2009.
29. S. Jetschke, S. Unger, A. Schwuchow, M. Leich, V. Reichel, and J. Kirchhof, "Photodarkening in Yb-Doped Silica Fibers: Influence of the Atmosphere During Preform Collapsing," *Proc. SPIE* **6873**, 68731G, 2008.
30. S. Unger, A. Schwuchow, S. Jetschke, V. Reichel, A. Scheffel, and J. Kirchhof, "Optical Properties of Yb-Doped Laser Fibers in Dependence on Codopants and Preparation Conditions," *Proc. SPIE* **6890**, 689016, 2008.

31. S. Girard, B. Tortech, E. Régnier, M. Van Uffelen, A. Gusarov, Y. Ouerdane, J. Baggio, P. Paillet, V. Ferlet-Cavrois, A. Boukenter, J.-P. Meunier, F. Berghmans, J. R. Schwank, M. R. Shaneyfelt, J. A. Felix, E. W. Blackmore, and H. Thienpont, "Proton- and Gamma-Induced Effects on Erbium-Doped Optical Fibers," *IEEE Trans. Nucl. Sci.* **54** (6), pp. 2426-2434, 2007.
32. B. Brichard, A. F. Fernandez, H. Ooms, M. Van Uffelen, and F. Berghmans, "Study of the Radiation-Induced Optical Sensitivity of Erbium and Aluminum-Doped Fibres," *Proceedings of the 7th European Conference on Radiation and its Effects on Components and Systems, RADECS 2003, IEEE*, 2003.
33. J. J. Koponen, M. J. Söderlund, H. J. Hoffman, D. A. V. Kliner, and J. Koplow, "Photodarkening Measurements in Large-Mode-Area Fibers," *Proc. SPIE* **6453**, 64531E, 2007.
34. M. N. Ott, "Radiation Effects Expected for Fiber Laser/Amplifier Rare Earth Doped Optical Fiber," Sigma Research and Engineering / NASA GSFC, Parts, Packaging and Assembly Technologies Office Survey Report, 2004.
35. H. Henschel, O. Köhn, H. U. Schmidt, J. Kirchhof, and S. Unger, "Radiation-Induced Loss in Rare Earth Doped Silica Fibres," *IEEE Trans. Nucl. Sci.* **45** (3), pp. 1552-1557, 1998.
36. G. M. Williams, M. A. Putnam, C. G. Askins, M. E. Gingerich, and E. J. Friebele, "Radiation Effects in Erbium-Doped Optical Fibres," *Electron. Lett.* **28** (19), pp. 1816-1818, 1992.
37. R. B. J. Lewis, E. S. R. Sikora, J. V. Wright, R. H. West, and S. Dowling, "Investigation of Effects of Gamma Radiation on Erbium-Doped Fibre Amplifiers," *Electron. Lett.* **28** (17), pp. 1589-1591, 1992.
38. J. Jasapara, M. Andrejco, D. DiGiovanni, and R. Windeler, "Effect of Heat and H_2 Gas on the Photo-Darkening of Yb^{+3} Fibers," *Conf. on Lasers and Electro-Optics/Quantum Electron. and Laser Sci. Conf. and Photon. App. Sys. Technolog*ies, Technical Digest, paper CTuQ5, 2006.
39. B. P. Fox, K. Simmons-Potter, W. J. Thomes, Jr., D. C. Meister, R. P. Bambha, and D. A. V. Kliner, "Temperature and Dose-Rate Effects in Gamma-Irradiated Rare-Earth Doped Fibers," *Proc. SPIE* **7095**, 70950B, 2008.